

C. Vericat · M. Wakisaka · R. Haasch · P. S. Bagus
A. Wieckowski

Binding energy of ruthenium submonolayers deposited on a Pt(111) electrode

Received: 10 March 2004 / Accepted: 6 April 2004 / Published online: 14 August 2004
© Springer-Verlag 2004

Abstract We investigated the $3d_{5/2}$ core-level binding energy of Ru in Ru nanoislands spontaneously deposited on a Pt(111) electrode [Pt(111)/Ru], and the binding energies of $3d_{5/2}$ iodine and $1s$ CO adsorbed on Pt(111)/Ru by the use of X-ray photoelectron spectroscopy. Both iodine and CO were used as surface probes of the electronic properties of Pt(111)/Ru. Little difference was found in the binding energy of Ru in Pt(111)/Ru and in Ru(0001). However, the addition of Ru to Pt(111) induces major changes in the core-level binding energies of chemisorbed iodine and CO as referenced to those adsorbed on Ru(0001). We conclude that the iodine $3d_{5/2}$ and CO $1s$ C core levels experience higher electronic charge on Pt(111)/Ru than on Ru(0001), suggesting a charge transfer from Pt to Ru, or to a Ru-I “surface molecule” within the deposit. The charge transfer from Pt to Ru is in agreement with the result of previous in situ electrochemical NMR investigations [P.K. Babu, H.S. Kim, A. Wieckowski, E. Oldfield (2003) *J. Phys. Chem. B* 107:7595] and confirms the general trend of reduction in the density of states of Pt due to alloying with Ru [J. McBreen, S. Mukerjee (1995) *J. Electrochem.*

Soc. 142:3399]. Theoretical calculations are in progress to further interpret the origin of the binding-energy shifts observed in this study.

Keywords X-ray photoelectron spectroscopy · Binding energy · Platinum · Ruthenium · Nanoislands · Iodine

Introduction

There is a need to better understand the promoting catalytic effect due to intermixing of metals in small molecule oxidation for fuel cells [1, 2, 3, 4, 5, 6, 7, 8, 9, 10, 11, 12]. In this regard, a frequently asked question is what is the best electronic-level observable that correlates with the fuel cell (and related) catalytic activity? On one hand, density functional theory indicates that the theoretical factor to correlate to the activity is the projected center of the d-band [13]. On the other hand, the frontier orbital theory of heterogeneous catalysis requires that Fermi level local densities of states (E_F -LDOS) account for electronic surface structure effects in the activity [14, 15].

The center of the d-band offers a direct indication of the reactivity (bond energies and hence activation energies) at sites of different geometry, and is indicative of modifications in catalytic properties due to intermixing of metals, for example, in a bimetallic catalyst. In such a case, the experimental observable to correlate with the d-band shift is the degree of the surface core level shift, or binding energy (BE) shift, offered in X-ray photoelectron spectroscopy (XPS) experiments [16]. Conversely, electrochemical (EC) NMR provides quantitative estimates of the E_F -LDOS [17]. The E_F -LDOS represent the availability of metal surfaces to donate/accept electrons to/from a metallic promoter to the host metal, and is a measure of the capacity of surface electrons excited with zero energy in responding to perturbations such as those by the addition of a second metal, and/or the addition of an adsorbate. While these two experimental approaches (BE

Dedicated to Zbigniew Galus on the occasion of his 70th birthday

C. Vericat · M. Wakisaka · A. Wieckowski (✉)
Department of Chemistry,
University of Illinois at Urbana-Champaign,
Urbana, IL 61801, USA
E-mail: andrzej@scs.uiuc.edu
Tel.: +1-217-3337943
Fax: +1-217-2448068

R. Haasch
Frederick Seitz Materials Research Laboratory,
University of Illinois at Urbana-Champaign,
Urbana, IL 61801, USA

P. S. Bagus
Department of Chemistry, University of North Texas,
Box 305070, Denton, TX 76203-5070, USA

Present address: M. Wakisaka
Clean Energy Research Center,
University of Yamanashi, Takeda 4,
400-8510, Kofu, Japan

and E_F -LDOS) may not be contradictory, experimental results can add credence to one of these, or to the two theoretical approaches. Ultimately, when a sufficient database of the BE observables is obtained, it will be available to theorists and will increase the predictive power of their computational methods in the future.

In this perspective, evidence was presented by this group [18] and by the Smotkin group [19] that Ru must be metallic to function as an effective catalyst promoter of Pt in the CO surface poison oxidation; a process of a vital importance in fuel cell catalysis. We therefore believe that it is imperative to understand Pt metal–Ru metal interactions on the electronic level [20]. As we are particularly interested in Ru nanoislands deposited on Pt single-crystal electrodes, we study in this report such nanostructured Pt(111)/Ru electrodes by the use of XPS. We generate the Pt/Ru surfaces by using the method of

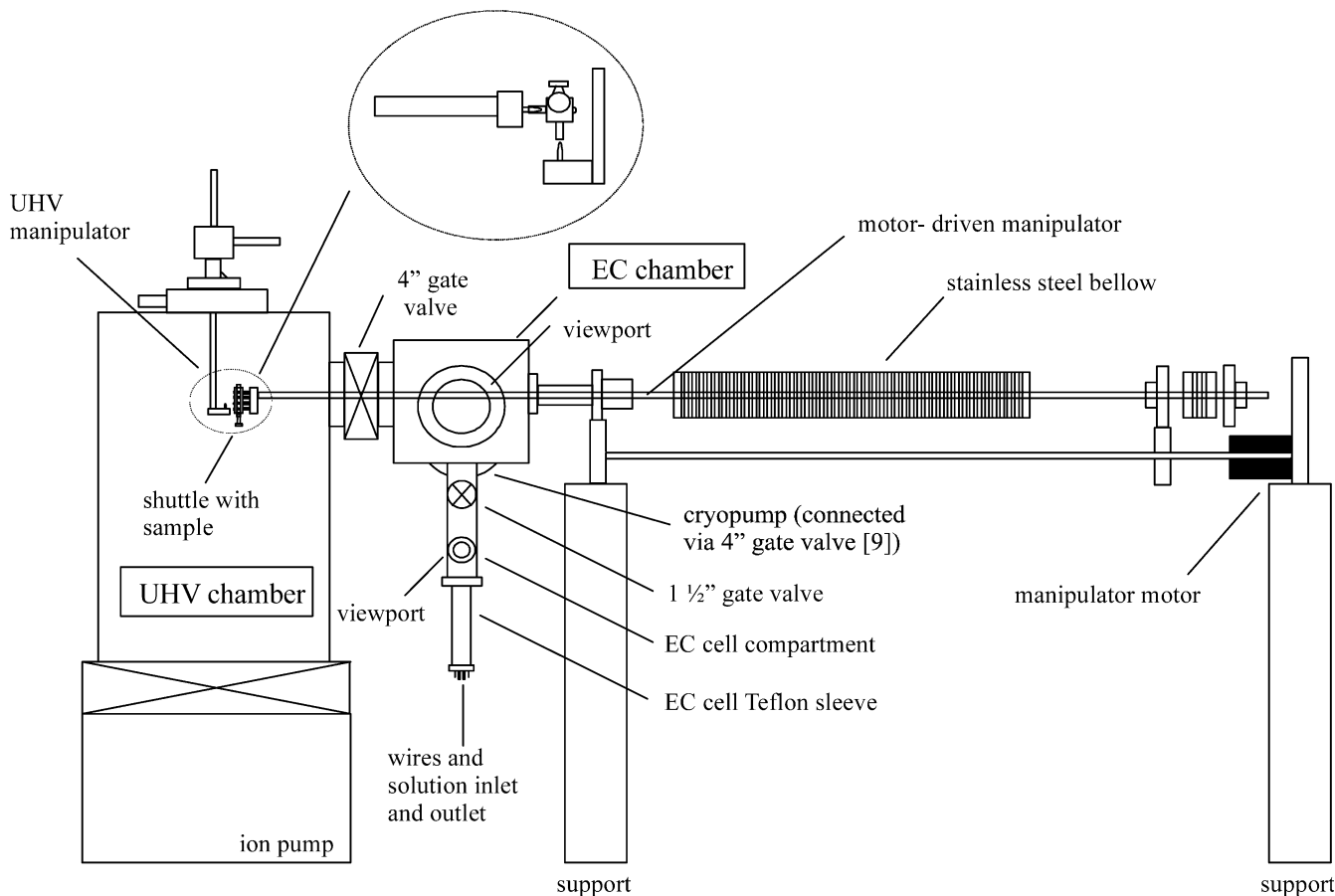
spontaneous deposition [21]. Namely, by immersion of Pt(111) in Ru admetal-containing solutions, the Pt surface becomes “decorated” by Ru nanoislands and/or clusters of adjustable packing density and height. The XPS measurements of such surfaces may allow us to investigate the BE difference (ΔBE) between Ru atoms in the Ru islands on Pt(111) and Ru surface atoms in the Ru(0001) substrate. We also studied iodine and CO adsorbed on Ru-island-covered Pt(111)/Ru surfaces. In the future, this work will be extended to other metal–metal systems of importance to fuel cell catalysis.

Materials and methods

Experimental

All experiments were carried out at ambient temperature (25 ± 2 °C). The chemicals used were sulfuric acid (GFS, double distilled from Vycor), $RuCl_3 \cdot xH_2O$ (Alfa Aesar), CO (Matheson, research purity), KI (Alfa Aesar), and Millipore water. Cyclic voltammetric measurements were carried out using a PAR 362 potentiostat and associated auxiliaries. The potentials were measured against a homemade Ag/AgCl electrode in Millipore water, but are reported versus a reference hydrogen electrode. Argon (S.J. Smith Welding Supply, ultrahigh purity) was used to maintain an inert atmosphere in the EC cell compartment (Fig. 1).

Fig. 1 Scheme showing the lateral view of the ultrahigh vacuum (UHV) electrochemical (EC) system. Depicted are from left to right: UHV manipulator, UHV chamber, EC chamber, EC cell and motor-driven (horizontal) manipulator with the shuttle and sample (now inside the UHV chamber). Inset (notice 180° rotation versus the demonstrated shuttle position in the UHV chamber): locking of the shuttle on the UHV manipulator after 90° rotation of the crystal. After transferring the shuttle from the horizontal to the UHV manipulator, the sample surface is at 30° with respect to the analyzer entrance slit (not shown). The angle between the sample surface and the incident X-ray beam is also 30°, and that between the analyzer and the incident X-ray beam is 90°



Pt(111)/Ru surfaces were obtained by the method of spontaneous deposition, as mentioned previously. The deposition was performed in 1 mM RuCl_3 and 0.1 M H_2SO_4 solutions for 5 min at an open circuit potential. After the spontaneous deposition, the electrode surface was rinsed with pure water to remove Ru-containing solution adhering to the Pt(111) surface, and the electrode was next subjected to a few voltammetric cleaning cycles at a scan rate of 50 mV/s between the onset of hydrogen evolution (at 0.08 V versus a reference hydrogen electrode) and the open circuit potential (0.90 V) in 0.1 M H_2SO_4 , before final reduction of the Pt/Ru deposit at 0.08 V for 30 min. This yielded metallic Ru coverage of around 0.2 monolayers. Higher Ru coverage (between 0.30 and 0.50 monolayers) was obtained by repeating the deposition/stabilization procedure, i.e., by performing a multiple spontaneous deposition, as reported before [21].

The single-crystal surfaces studied here, which terminated disk-shaped crystals of Pt and Ru, were 10 [Pt(111)] and 6 mm [Ru(0001)] in diameter. The Pt(111) and Ru(0001) single crystals were obtained from Accu-met Materials and MaTeck, respectively. Pt wires spot-welded to the back of the crystals connected the crystals to the sample holder (the shuttle in Fig. 1). Remnants of copper present on the back of the crystal were removed with nitric acid before a crystal was connected to the shuttle. The crystal surface in ultrahigh vacuum (UHV) was cleaned by argon ion bombardment and subsequently by hot argon ion bombardment, and finally it was annealed at high temperature in UHV (including, when needed, annealing in an oxygen atmosphere at 10^{-8} Torr). The surface cleanliness was controlled by XPS.

XPS instrument

The EC UHV-XPS instrument used for this study was an enhanced version of the Auger/low-energy electron diffraction design reported in Ref. [10]. New and key features of this design are the following: a "shuttle" is added as a vehicle to transfer the crystal between two instrument chambers (Figure 1) and two manipulators are used instead of one. The manipulators deliver the sample (e.g., a Pt or Ru single crystal) to the UHV chamber from the EC chamber, or take the sample back from UHV to the EC cell (Fig. 2). After the crystal is positioned in front of the electron-energy analyzer associated with the XPS spectrometer, the manipulator is withdrawn and a 4-in. gate valve is closed, thus isolating the main UHV chamber from the EC part of the instrument. (The latter, despite active pumping by the cryopump of the EC chamber, may still have some memory of the argon gas and water vapor from the previous EC phase of the experiment.)

While the horizontal manipulator is motor-driven, the UHV manipulator is manual and always at UHV (Fig. 1). A liquid helium cryopump is used as a frontier

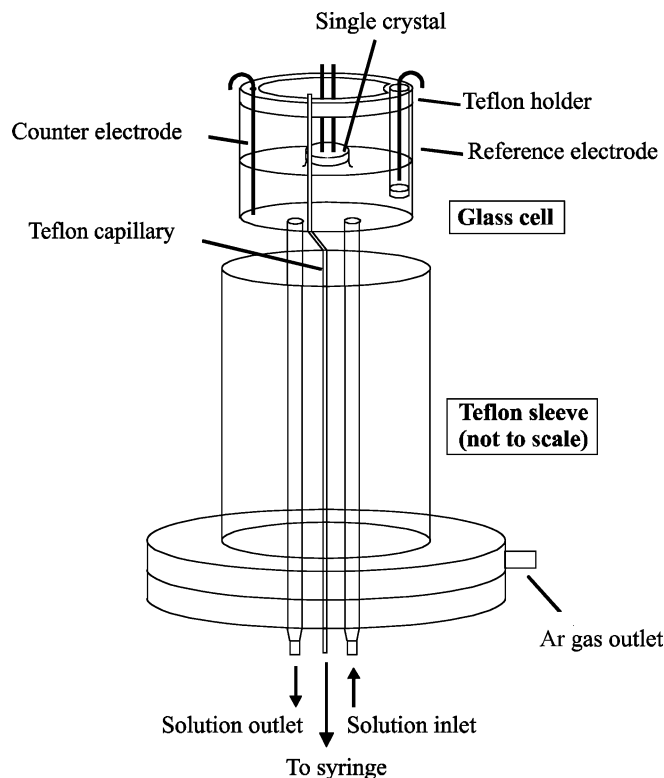


Fig. 2 EC cell incorporated into the UHV system with a single crystal in a meniscus configuration

pump (after prepumping by liquid nitrogen sorption pumps). The cryopump is connected to the chamber via a 4-in. gate valve. The UHV chamber is pumped by ion pumps and may additionally be pumped by a titanium sublimation pump [10]. The base pressure of the UHV-XPS chamber after a prolonged bakeout is 1×10^{-11} Torr. The shuttle design allows high-temperature annealing of the crystal up to 1,000 °C.

The EC cell (Fig. 2) has its own compartment (Fig. 1) that is kept under an ultrapure argon atmosphere while surface characterization of the electrode is carried out in UHV, or when the crystal is transferred between chambers. The compartment is connected to the EC chamber through a 2-in. gate valve. The important part of the EC cell design (Fig. 2) is the solution inlet and outlet that facilitate rinsing of the working electrode without losing the electrode potential control (wherever such a potentiostatic rinsing procedure is required), as reported before [10].

Following surface preparation in UHV, the 4-in. gate valve is opened, and the shuttle with the attached sample is transferred to the EC chamber. In the meantime, the EC cell is filled with argon-deaerated sulfuric acid solution. With the gate valves closed, the EC chamber is brought to atmospheric pressure with argon (vented via an argon leak and a bubbler). The 1.5-in. gate valve is then opened, and the cell, installed in the Teflon sleeve (Fig. 1), is pushed upward into the EC chamber interior. The sample surface is then connected to the solution via

a meniscus configuration (Fig. 2) for the voltammetric characterization and/or Ru deposition, as described in the next section of this paper. Argon overpressure keeps air effectively out at any phase of this experiment before the system is evacuated. After completion of the EC treatment, the cell is withdrawn below the 1.5-in. valve leaving the electrode, with the hanging drop of water, exposed to ultrapure argon. The electrode-manipulator arm is then tilted to a near horizontal position and the water is collected at the edge of the crystal. Water is then easily removed from the crystal edge via thin Teflon tubing attached to a syringe. Water removal reduces the time needed for bringing the EC chamber to the UHV pressure range (in around 10 min) after which the sample is transferred to the UHV chamber.

The surfaces were analyzed by XPS, usually at around 10^{-9} Torr, using an ESCA M-Probe high-resolution, multichannel hemispherical electron analyzer (Surface Science Instruments) and an ion gun for surface cleaning. For the XPS characterization, a monochromatic Al $K\alpha$ line ($h\nu=1,486.6$ eV) operated at 110 W was used as the excitation source. The photoelectron energy was measured using the fixed analyzer transmission (constant pass energy) mode with a constant pass energy of 25 eV, and the size of the incident X-ray beam was 800 μm . An S-Probe version of the 1.36 ESCA software (Fisons Instruments) was used, and spectral peaks were fitted using a mixed Gaussian–Lorentzian line shape and Shirley baselines. The BEs measured were corrected with the standard binding energies of Au recommended by the National Institute of Standards and Technology.

Results and discussion

Cyclic voltammetry

Cyclic voltammograms (CVs) of a clean Pt(111) electrode obtained in 0.1 M H_2SO_4 at 50 mV/s after the UHV surface preparation (as described previously) are shown in Fig. 3a. The CVs demonstrate the high quality of the electrode surface, and confirm the cleanliness of our EC system and a contamination-free UHV-electrochemistry transfer procedure. By introducing approximately 0.5 monolayers of spontaneously deposited Ru to the Pt(111) surface [21, 22, 23, 24] (see earlier) two characteristic changes in the original voltammetric profile are observed (Fig. 3b). First, the negative- and positive-going spikes at 0.49 V (belonging to the anomalous region [25]) are significantly suppressed [26] and, second, the pseudocapacitive current in the 0.50–0.85-V region is enlarged, characteristic of a Ru-type electrode [26, 27].

The CV of a Ru(0001) surface in 0.1 M H_2SO_4 (Fig. 3c) shows features not typical of the Pt(111)/Ru surface studied. For example, Ru surface oxidation occurs as early as (approximately) 0.6 V, and oxide reduction occurs at two negative-going cyclic

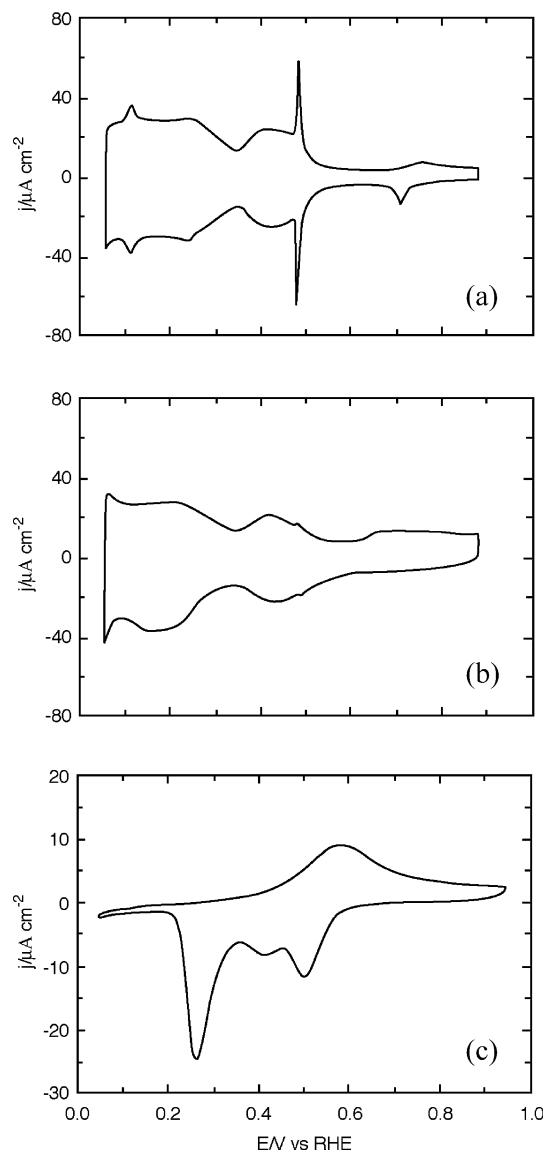


Fig. 3 Cyclic voltammograms taken in the EC cell of Fig. 2 for **a** clean Pt(111), **b** Pt(111)/Ru with 0.5 monolayers of Ru added following the treatment described in the text, and **c** clean Ru(0001), all in 0.1 M H_2SO_4 solution. Scan rates were 50 mV/s for **a** and **b** and 10 mV/s for **c**

voltammetry peaks, at 0.5 and 0.25 V, with an in-between peak at 0.45 V, all at 10 mV/s. The data in Fig. 3c also confirm previous data obtained by Wang et al. [28, 29, 30]. A successive cyclic at 10 mV/s did not induce any noticeable change in the voltammetric morphology (Figure 3c), confirming previous observation that repetitive cyclic voltammetric cycling does not bring surface disorder to the Ru(0001) electrode surface [28].

For the CO stripping cyclic voltammetry measurements, CO adsorption was carried out from CO-saturated 0.1 M H_2SO_4 solutions at 0.1, 0.28, and 0.25 V, respectively. This was followed by the solution replacement using an argon-pressurized flask containing 0.1 M H_2SO_4 solution to completely remove the dissolved CO while holding the electrode at the potential of choice. The

CO-stripping profiles from Pt(111) [31], Pt(111)/Ru [32] in Fig. 4 and Ru(0001) [29] in Figure 5 (to clean 0.1 M H₂SO₄ solution) indicate that the coverage of CO in all cases is close to 0.75 monolayers, confirming previous data [11, 33, 34, 35, 36, 37, 38]. Owing to the high Ru and CO coverage in this experiment, the CV of the CO oxidation on the Pt(111)/Ru in Fig. 4 is very similar to that reported previously [32]. Otherwise, at a Ru coverage of 0.2 monolayers, two voltammetric stripping maxima are found [32, 39], indicating that part of the CO adlattice is chemisorbed onto the Ru islands deposited on Pt(111), while the more positive peak originates from CO chemisorbed on the Ru-free Pt(111) sites [of the Pt(111)/Ru electrode]. Owing to Ru added to Pt(111), the peak located at a more positive potential, 0.67 V, is shifted in the negative direction with respect to the CO stripping from pure Pt(111), as already well known [11].

The data in Fig. 5 indicate that it is possible to remove CO from the Ru(0001) electrode but with considerable difficulty. It takes at least six cyclic voltammetry scans to completely remove the CO in the potential range studied. This obvious difficulty in performing the CO removal reaction [29] is in contrast to the apparent ease of the CO stripping on the Ru islands on Pt(111) [9, 11, 32, 39, 40] (Fig. 4). Apparently, the prerequisite for the CO oxidative removal from Ru of hexagonal geometry is the presence of the underlying Pt support that modifies the electronic (or geometric) properties of Ru surface atoms [7, 9, 41] and allows for a facile nucleation of CO in its drive to become oxidized to CO₂. From the data in Fig. 5 we also conclude that CO chemisorption on Ru(0001) passivates the Ru electrode and the CO passive monolayer film can be stripped off in a partial oxidation reaction under successive cyclic voltammetric treatment.

XPS measurements of Ru

XPS measurements were first carried out with the Ru(0001) surface to establish the BE reference for metallic Ru deposited on the Pt(111) electrode. A typical

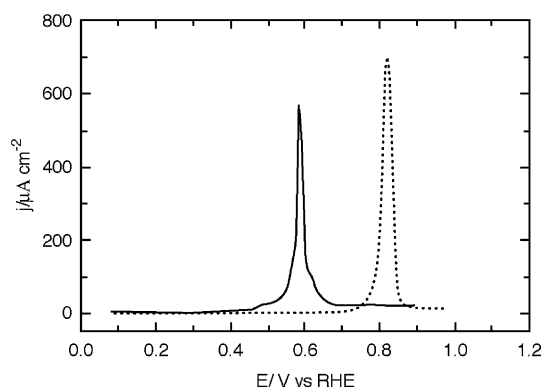


Fig. 4 Stripping of a CO adlayer from Pt(111) (dotted line) and from Pt(111)/Ru with 0.5 monolayers of Ru (solid line) in a clean 0.1 M H₂SO₄ solution. The scan rate was 50 mV/s

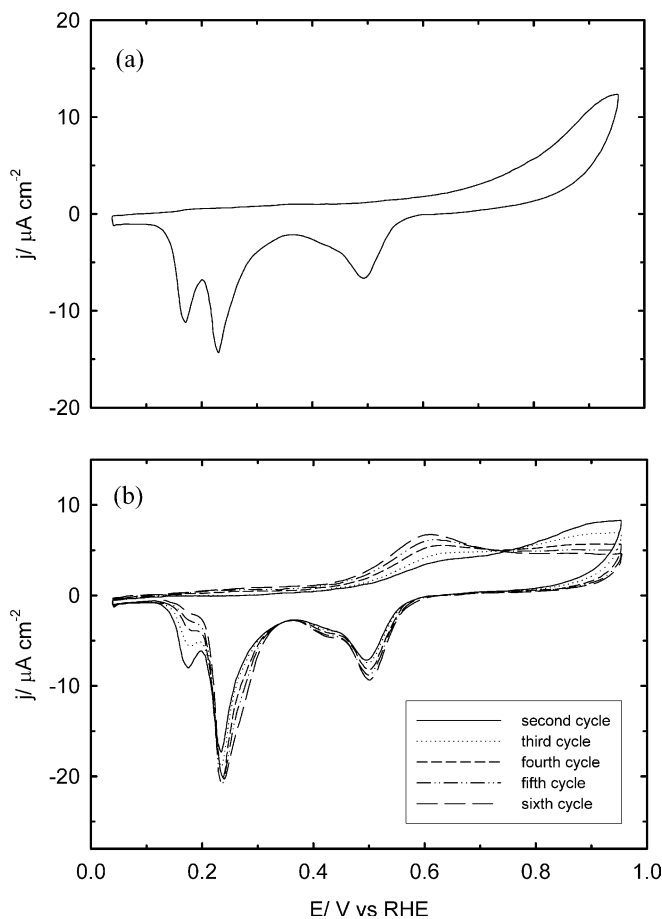


Fig. 5 Stripping of a CO adlayer from Ru(0001) in a clean 0.1 M H₂SO₄ solution: **a** first cycle; **b** subsequent cycles. The scan rate was 10 mV/s

Ru 3d spectrum, with 3d_{3/2} and 3d_{5/2} split by approximately 4.1 eV, of such a Ru(0001) surface is shown in Fig. 6a. The average Ru 3d_{5/2} BE was 280.1 ± 0.1 eV at 0.9 eV full width at half maximum, in a perfect agreement with the literature value [42].

XPS measurements were next conducted with sub-monolayers of Ru added to the UHV-prepared Pt(111) surface by spontaneous deposition, as described previously. A typical XPS spectrum of the Pt(111)/Ru surface is shown in Fig. 6b. The data in this figure were obtained after a considerable reduction of the original spontaneously obtained deposit, see Experimental. The Ru region is well fitted with a single doublet, showing that Ru forms other than metallic Ru, such as RuO₂ and RuO₃ [43], or C contaminants are not present on the Pt(111) surface. We found that the BE of metallic Ru is independent of coverage in the range 0.2–0.5 monolayers. Notably, the Ru 3d_{5/2} BE value is 280.1 ± 0.1 eV; the same, within experimental error, as obtained for the clean Ru(0001) surface, which shows the experimental ΔBE between Ru atoms in the Ru islands on Pt(111)/Ru and Ru atoms on/in Ru(0001) is very small. The ΔBE may be small per se, or there may exist some effects specific to small Ru nanoislands that offset the BE

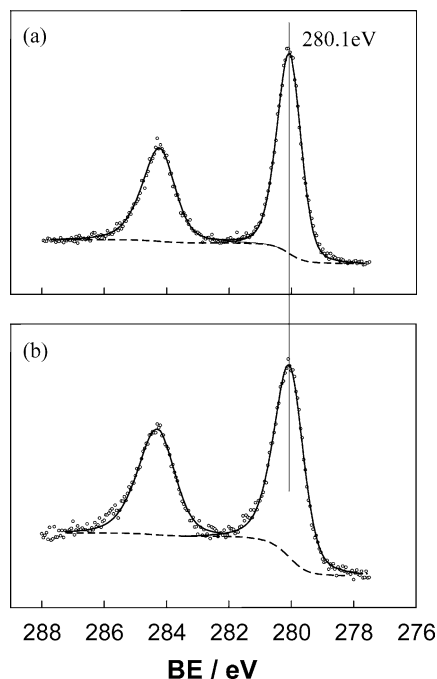


Fig. 6 Typical Ru $3d_{5/2}$ spectra for **a** clean Ru(0001) and **b** the Ru species on Pt(111) obtained after the treatment described in the text (0.5 monolayers of Ru). The binding energy (BE) is 280.1 eV in both spectra

change [44]. For instance, the Ru BE shifts on these two surfaces are small because of the compensation between the strain factor within the nanoislands and the charge transfer between Ru and Pt [45, 46, 47]. Theoretical methods have been developed [45] to enable us to identify the initial and final state effects that contribute to the Δ BE shifts in foreign metal nanoislands on host metal surfaces [47]. This will be pursued. Notice that no consideration was given in this paper to the core level shifts between the Ru surface and bulk Ru atoms either [48, 49]. We will address this issue in the next study from this laboratory.

Notably, XPS of a broad range of foreign metal adlattices on a host metal surface was explored by Liu et al. [48, 49]. In contrast to this quoted work, we investigated essentially monoatomic islands, approximately 2–3-nm wide [21], which do not belong to the 2D adlattice category studied before. As we indicated in the Introduction, these small adislands are formed spontaneously, and have their own unit cell structures without a fixed relation to each other. Moreover, they display different strain behavior versus metal/metal adlattices studied by XPS to date. We believe we have initiated new core level research on an attractive class of surfaces, also of strong relevance to modern topics in fuel cell catalysis.

BE shifts of adsorbed iodine

As indicated in the Introduction, we measured the BEs of the surface iodine and CO deposited on the

Ru-island-covered Pt(111) surfaces, and on Ru(0001) (of the same hexagonal geometry). The strategy was to study the core-level behavior of iodine and CO adsorbed on these two purely metallic surfaces (Fig. 7). XPS data for chemisorbed iodine will be discussed next, and those for chemisorbed CO in the next subsection of this paper.

Iodine adsorption on the Pt(111), Pt(111)/Ru, and Ru(0001) surfaces was performed at 0.2 V in 0.1 M H_2SO_4 solutions containing KI at different KI concentrations. In order to obtain saturation iodine coverage (0.43 monolayers), a 1 mM KI solution was used and the iodine adsorption was carried out for 2 min. For lower iodine coverage, the adsorption was carried out in 10 μM KI solution for 30 min at potentials lower than 0.2 V.

A representative $3d_{5/2}$ XPS spectrum for Pt(111)–I surfaces at the iodine coverage of 0.43 monolayers [50] is shown in Fig. 8a, small circles. The peak-fitting (dashed lines) yields two components, at 619.4 and at 618.4 eV, in agreement with the literature values [51, 52, 53]. Iodine on Pt(111) is known to form a $(\sqrt{7}\times\sqrt{7})\text{R}19.1^\circ$ lattice with two iodine atoms in threefold hollow sites and with one iodine atom in an on-top site per unit cell [50, 52]. The high BE component is assigned to a threefold hollow of iodine on Pt(111), while the one at the lower BE originates from the on-top iodine [52]. Our results shown in Fig. 8a are consistent with the 2:1 threefold-to-on-top ratio, as in Refs. [51, 52, 53]. At a lower coverage of iodine, surface iodine forms a $(\sqrt{3}\times\sqrt{3})\text{R}30^\circ$ adlattice only, and all iodine atoms are in threefold hollow sites, and this yields a single BE value easily fitted to a single component at 619.5 eV (Fig. 9).

For Pt with Ru, and for Ru(0001), the iodine-covered surfaces were obtained by electrode immersion in a 0.1 M H_2SO_4 solution containing KI at different KI concentrations. As previously, the electrode was rinsed

Probing the electronic structure of Ru nano-islands With atoms or molecular adlayers

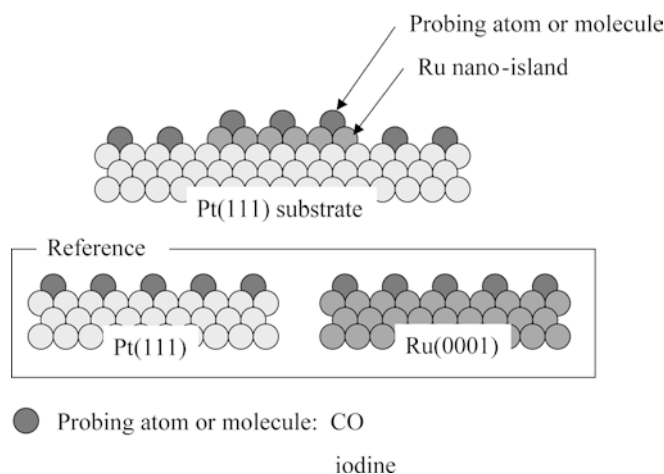


Fig. 7 Scheme of the strategy used in this paper to study the electronic properties of the bimetallic Pt/Ru surfaces

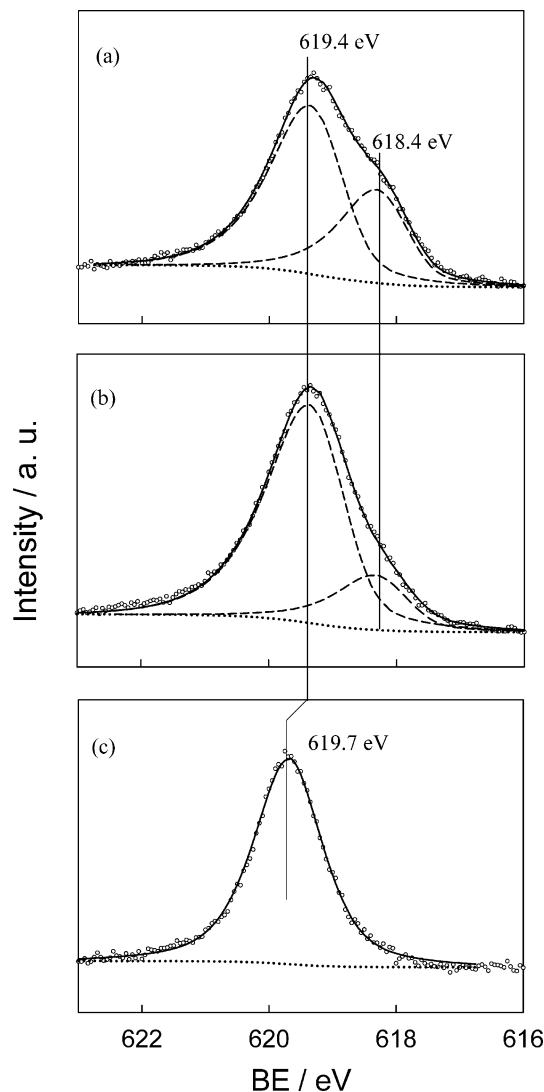


Fig. 8 Iodine X-ray photoelectron spectroscopy (XPS) $3d_{5/2}$ spectra for high coverage of iodine on **a** Pt(111), **b** Pt(111)/Ru with 0.5 monolayers of Ru, and **c** Ru(0001). The spectrum in **a** can be fitted with two components: the one at higher BE corresponds to iodine in threefold hollow sites and the other one corresponds to iodine on top sites. The spectrum in **b** can be fitted with three components: two at the same BE corresponding to iodine in hollow sites of Pt(111) and Ru(0001) and one at higher BE for iodine on-top sites of Pt(111). The spectrum in **c** can be fitted with only one component. A shift of 0.3 eV between the higher BE components of **b** and **c** can be clearly observed

to remove any remnants of the solution iodine species adhering to the electrode surface. At a saturation concentration of iodine on both Pt(111)/Ru and Ru(0001), the typical data are those shown in Fig. 8b and c, respectively [for the Ru coverage on Pt(111) of 0.5 monolayers]. The three expected components that are fitted are as follows. The one at 618.4 eV is attributed to the on-top iodine on Pt(111). There are also two threefold components at the same BE (619.4 eV): one is attributed to the threefold hollow iodine on Pt(111) and the other to iodine on Ru [deposited on Pt(111)]. We also found that as the Ru coverage on Pt(111) increased

the component at 618.4 eV [the on-top iodine on Pt(111)] decreased.

As mentioned already, the $3d_{5/2}$ peak of iodine on the Ru(0001) electrode is depicted in Fig. 8c. There is a single component at 619.7 eV from the threefold hollow iodine on the Ru(0001) surface, consistent with the literature value [54]. Comparing the data obtained with chemisorbed iodine on Ru from Pt(111)/Ru with the data on Ru(0001)-I, we find a BE difference of 0.34 V. Spectra for the iodine $3d_{5/2}$ peak that correspond to low iodine coverage (around 0.2 monolayers) on Pt(111), Pt(111)/Ru, and Ru(0001) are shown in Fig. 9. The left spectrum is for Ru(0001)-I and the right spectra are for the Pt-based surfaces. The spectrum of iodine on Ru(0001) at low iodine coverage shows only one component, at 619.8 eV. For Pt(111)-I at low iodine coverage, iodine adsorbs as a $(\sqrt{3}\times\sqrt{3})R30^\circ$ lattice, and the spectrum overlaps with those for iodine on Pt(111)/Ru-I. The peak can be fitted with one component, at 619.5 eV, assigned to iodine atoms in the threefold hollow sites. The XPS spectra from iodine on Pt(111)/Ru are Ru-coverage-independent (from 0.09 and 0.36 monolayers). A slight (less than 0.1 eV) difference in the BE of iodine on Pt or Ru with iodine coverage was previously observed and attributed to the final-state adsorbate-adsorbate interactions [52].

The data in Fig. 9 show that chemisorbed iodine on the Ru part of Pt(111)/Ru has a lower BE by 0.3 eV compared with the BE of iodine chemisorbed on Ru(0001), in good agreement with the difference found in Fig. 8 for higher iodine coverage. A possible interpretation of this effect is that the iodine core level experiences higher electronic charge when it is chemisorbed on Pt(111)/Ru than it does on Ru(0001), suggesting an electron charge transfer from Pt to Ru upon

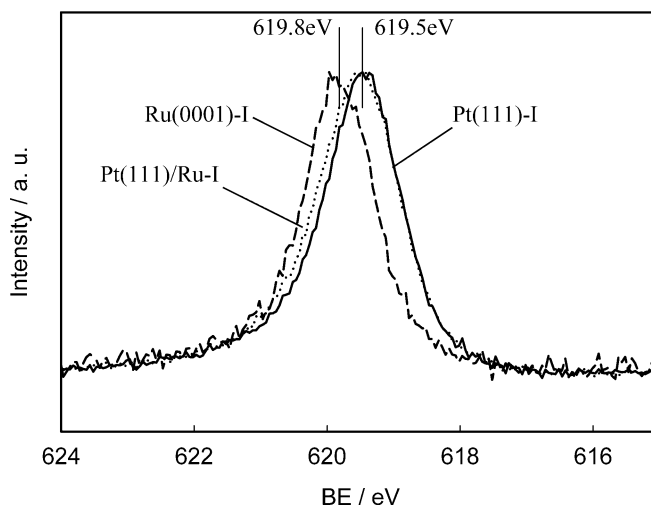


Fig. 9 XPS spectra of the iodine $3d_{5/2}$ peak corresponding to low coverage iodine adlayers on different substrates. Iodine on Pt(111) (solid line), iodine on Ru(0001) (dotted line), Ru on Pt(111), 0.5 monolayers of Ru (dashed dotted line). A shift of 0.3 eV between the spectra for Ru on Pt(111) and Ru(0001) can be observed

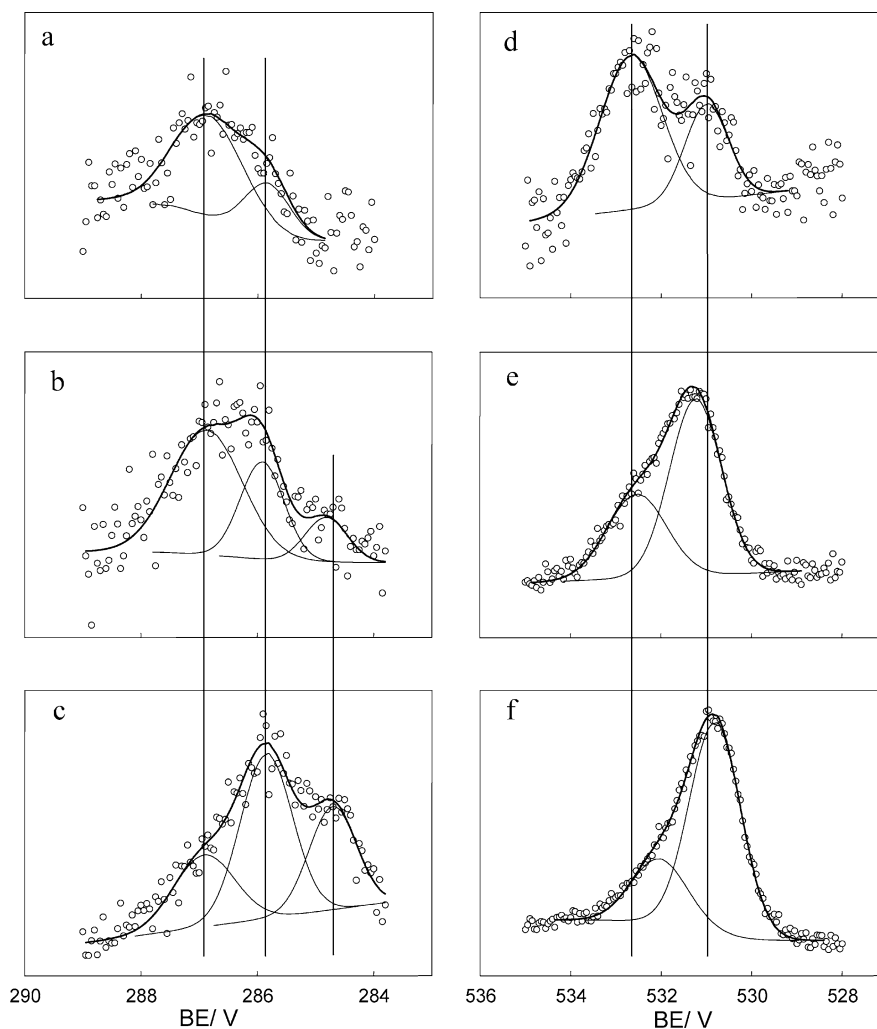
deposition of Ru on Pt. However, it must be a collective electron density shift from the Pt surface to the Ru–I surface molecule, as the BE of Ru also decreases by around 0.2 eV at high iodine coverage (and by around 0.1 eV at low iodine coverage). Thus, the full Ru–I “surface molecule” seems to behave as an electron density sink, or at least there is an electron-attracting Ru–I bond acting on the support Pt surface atoms. The charge transfer from Pt to Ru is in agreement with the result of previous in situ investigations: X-ray absorption near-edge spectroscopy and EC NMR [55] studies. Cluster model theoretical studies of the BE shifts are in progress to interpret and to clarify further the origin of the observed shifts; for discussions of the application of this theoretical approach for the analysis of BE shifts, see Ref. [45] and references therein. The principle objective of the calculations is to relate BE shifts to the electronic state of the Ru nanoislands on Pt and to identify the changes in the electronic structure of the islands from that of Ru(0001) surfaces. A vital feature of the calculations is that they provide a means to distinguish the chemically interesting initial state contributions to the BE shifts from the final state relaxation, or

screening, contributions to the shifts that are less important for chemical properties. The consequences for the shifts of the BEs arising from lattice strain in the Ru islands [47] as well as from variations of the adsorbate–substrate bond distance [56] will be investigated, from a quantitative perspective.

BE shifts of adsorbed CO

It is well known that CO on both Pt(111) [57, 58] and Ru(0001) [59, 60] is adsorbed in an upright position with the carbon directly coordinated to the surface. It is shown in Fig. 10a that the C 1s BE for CO on Pt(111) is 286.9 eV for the linear and 285.9 eV for the bridge-bonded CO, in agreement with the literature values [57, 61]. The peak ratios of the two forms are around 3:1, as expected. As with chemisorbed iodine discussed previously, addition of Ru to Pt(111) induces major changes in the XPS spectra of chemisorbed CO (Fig. 10b). The development between Fig. 10a and b, and then with Fig. 10c when the Ru coverage increases, is the growth of the XPS C 1s intensity from CO on the Ru phase

Fig. 10 XPS spectra for **a–c** C 1s and **d–f** O 1s for CO adlayers on different substrates: **a, d** Pt(111); **b** Pt(111)/Ru with 0.1 monolayers of Ru; **c, e** Pt(111)/Ru with 0.5 monolayers of Ru; **f** Ru(0001)



deposited on Pt(111), which is at 284.7 eV. The point to notice, however, is that the Ru(0001)-CO reference is at 285.7 eV [62], i.e., the BE of the C 1s from CO on Pt(111)/Ru (adsorbed on the Ru phase) is lower by 1 eV than that from the C 1s from CO chemisorbed on Ru(0001) [62, 63, 64], consistent with the iodine data discussed earlier. There is also a small BE shift toward a lower Ru $3d_{5/2}$ BE in Pt(111)/Ru-CO with respect to that for bare Pt(111)/Ru, echoing the behavior for iodine and Ru atoms sandwiched between Pt and iodine. However, the XPS data for O 1s from CO do not obviously add credence to the trends established with iodine (Fig. 10d-f), and a more advanced interpretation using similar theoretical cluster model studies as those described previously for the iodine BE shifts is awaited. Such and similar data will be interpreted theoretically as they relate to some key issues from the IR characterization of Pt(*hkl*)/Ru-CO surfaces [4, 65] and overall to key topics in fuel cell catalysis.

Conclusions

We have studied the core-level behavior of Ru atoms in Ru nanoislands on Pt(111) and Ru atoms in Ru(0001). The difference in the Ru BE shifts on these two surfaces is very small, possibly because of the compensation between the strain factor within the nanoislands and the charge transfer between Ru and Pt. We have also studied core levels of adsorbed iodine and CO used as surface probes to explore the electronic state of such Ru-island-covered Pt surfaces. We conclude that the $3d_{5/2}$ iodine and C 1s CO core levels experience a higher electronic charge on Pt(111)/Ru than on Ru(0001), suggesting a charge transfer from Pt to Ru upon deposition of Ru on Pt, as concluded earlier from EC NMR and X-ray absorption near-edge spectroscopy measurements. However, this must be a collective electron density shift from the Pt substrate to the Ru-I (or Ru-C) surface chemical bond, as the BE of Ru is also reduced owing to Ru interactions with the Pt atoms underneath. The core level shifts observed in this report reveal differences in the electronic structure of the surfaces studied that may help us to understand the nature of these Ru nanoislands on Pt and their influence on catalytic activities, from the perspective of electronic effects in heterogeneous electrocatalysis. Theoretical calculations are in progress to interpret further the origin of the observed BE shifts with regards to possible changes in the electronic state of Ru nanoislands due to interactions of Ru with Pt.

Acknowledgements This work was carried out in the Center for Microanalysis of Materials, University of Illinois, which is partially supported by the U.S. Department of Energy under grant DEFG02-91-ER45439. This work was also supported by the National Science Foundation Grant CHE 9985837. The authors acknowledge the original design of the electrochemistry-XPS transfer system by P. Mrozek, currently at Micron Technology, Boise, ID 83707, USA.

References

1. McBreen J, Mukerjee S (1995) *J Electrochem Soc* 142:3399
2. Wieckowski A, Savinova E, Vayenas C (2003) *Catalysis and electrocatalysis at nanoparticle surfaces*. Dekker, New York, p 1
3. Park S, Wieckowski A, Weaver MJ (2003) *J Am Chem Soc* 125:2282
4. Friedrich KA, Geyzers KP, Dickinson AJ, Stimming U (2002) *J Electroanal Chem* 524:261
5. Iwasita T (2002) *Electrochim Acta* 47:3663
6. Markovic NM, Ross PN (2002) *Surf Sci Rep* 45:121
7. Waszczuk P, Lu GQ, Wieckowski A, Lu C, Rice C, Masel RI (2002) *Electrochim Acta* 47:3637
8. Waszczuk P, Solla-Gullon J, Kim HS, Tong YY, Montiel V, Aldaz A, Wieckowski A (2001) *J Catal* 203:1
9. Tong YY, Rice C, Wieckowski A, Oldfield E (2000) *J Am Chem Soc* 122:1123
10. Chrzanowski W, Wieckowski A (1999) In: Wieckowski A (ed) *Interfacial electrochemistry: theory, experiment, and applications*. Dekker, New York, p 937
11. Koper MTM, Lukkien JJ, Jansen APJ, van Santen RA (1999) *J Phys Chem B* 103:5522
12. Reddington E, Sapienza A, Gurau B, Viswanathan R, Sarangapani S, Smotkin E, Mallouk T (1998) *Science* 280:1735
13. Hammer B, Norskov JK (2000) *Adv Catal* 45:71
14. Hoffmann R (1988) *Rev Mod Phys* 60:601
15. Mavrikakis M, Hammer B, Norskov JK (1998) *Phys Rev Lett* 81:2819
16. Norskov JK, Wieckowski A (organizers), workshop on: "Theory and Surface Measurements of Fuel Cell Catalysis", Center for Atomic-Scale Materials Physics, University of Denmark, Lyngby, Denmark, June 16-18, 2003
17. Babu PK, Oldfield E, Wieckowski A (2003) In: Vayenas CG, Conway BE, White RE (eds) *Modern aspects of electrochemistry*. Kluwer/Plenum, New York, p 1
18. Kim H, Rabelo de Moraes I, Tremiliosi-Filho G, Haasch R, Wieckowski A (2001) *Surf Sci* 474:L203
19. Viswanathan R, Hou G, Liu R, Bare S, Modica F, Mickelson G, Segre C, Leyarovska N, Smotkin E (2002) *J Phys Chem B* 106:3458
20. Rodriguez JA, Goodman DW (1992) *Science* 257:897
21. Crown A, Johnston C, Wieckowski A (2002) *Surf Sci* 506:L268
22. Chrzanowski W, Wieckowski A (1997) *Langmuir* 13:5974
23. Crown A, Moraes IR, Wieckowski A (2001) *J Electroanal Chem* 500:333
24. Crown A, Wieckowski A (2001) *Phys Chem Chem Phys* 3:3290
25. Clavilier J (1999) In: Wieckowski A (ed) *Interfacial electrochemistry: theory, experiment, and applications*. Dekker, New York 231-248
26. Herrero E, Feliu JM, Wieckowski A (1999) *Langmuir* 15:4944
27. Conway BE (1995) *Prog Surf Sci* 49:331
28. Wang JX, Marinkovic NS, Zajonz H, Ocko BM, Adzic RR (2001) *J Phys Chem B* 105:2809
29. Marinkovic NS, Wang JX, Zajonz H, Adzic RR (2000) *Electrochem Solid State Lett* 3:508
30. Marinkovic NS, Wang JX, Zajonz H, Adzic RR (2001) *J Electroanal Chem* 500:388
31. Zurawski D, Wasberg M, Wieckowski A (1990) *J Phys Chem* 94:2076
32. Lu GQ, Waszczuk P, Wieckowski A (2002) *J Electroanal Chem* 532:49
33. Gomez R, Feliu JM, Aldaz A, Weaver MJ (1998) *Surf Sci* 410:48
34. Feliu JM, Orts JM, Fernandezvega A, Aldaz A, Clavilier J (1990) *J Electroanal Chem* 296:191
35. Feliu JM, Orts JM, Gomez R, Aldaz A, Clavilier J (1994) *J Electroanal Chem* 372:265
36. Santos E, Leiva EPM, Vielstich W (1991) *Electrochim Acta* 36:555
37. Lebedeva NP, Koper MTM, Feliu JM, van Santen RA (2002) *J Phys Chem B* 106:12938-12047

38. Lebedeva NP, Koper MTM, Herrero E, Feliu JM, van Santen RA (2000) *J Electroanal Chem* 487:37
39. Massong H, Wang HS, Samjeske G, Baltruschat H (2000) *Electrochim Acta* 46:701
40. Gasteiger HA, Markovic N, Ross PN, Cairns EJ (1993) *J Phys Chem* 97:12020
41. Babu PK, Kim HS, Wieckowski A, Oldfield E (2003) *J Phys Chem B* 107:7595
42. Powell CJ (1995) *Appl Surf Sci* 89:141
43. Kim H, de Moraes IR, Tremiliosi G, Haasch R, Wieckowski, A. (2001) *Surf Sci* 474:L203
44. Egelhoff WA (1986) *Surf Sci Rep* 6:253
45. Bagus PS, Illas F, Pacchioni G, Parmigiani F (1999) *J Electron Spectrosc Relat Phenom* 100:215
46. Liu G, Davis KA, Meier DC, Bagus PS, Goodman DW, Zajac GW (2003) *Phys Rev B* 68:035406
47. Richter B, Kuhlenbeck H, Freund H-J, Bagus PS (2004) *Physical Review Letters* 93:026805/1–026805/4
48. Liu G, St Clair TP, Goodman DW (1999) *J Phys Chem B* 103:8578
49. Liu G, Davis KA, Meier DC, Bagus PS, Goodman DW, Zajac GW (2003) *Phys Rev B* 68:035406
50. Lu F, Salaita GN, Baltruschat H, Hubbard AT (1987) *J Electroanal Chem* 222:305
51. Diczno SB, Wertheim GK, Buchanan DNE (1982) *Surf Sci* 121:411
52. Diczno SB, Wertheim GK, Buchanan DNE (1984) *Phys Rev B* 30:553
53. Jo SK, White JM (1992) *Surf Sci* 261:111
54. Kis A, Smith KC, Kiss J, Solymosi F (2000) *Surf Sci* 460:190
55. Babu PK, Kim HS, Oldfield E, Wieckowski A (2003) *J Phys Chem B* 107:7595–7600
56. Parmigiani F, Pacchioni G, Brundle CR, Fowler DE, Bagus PS (1991) *Phys Rev B* 43:3695
57. Norton PR, Goodale JW, Selkirk EB (1979) *Surf Sci* 83:189
58. Rodriguez JA, Truong CM, Goodman DW (1992) *J Chem Phys* 96:7814
59. Fuggle JC, Steinkilberg M, Menzel D (1975) *Chem Phys* 11:307
60. Riedmuller B, Ciobica IM, Papageorgopoulos DC, Frechard F, Berenbak B, Kley AW, van Santen RA (2001) *J Chem Phys* 115:5244
61. Ramstad A, Strisland F, Raaen S, Borg A, Berg C (1999) *Surf Sci* 440:290
62. Fohlisch A, Hasselstrom J, Karis O, Vaterlein P, Martensson N, Nilsson A, Heske C, Stichler M, Keller C, Wurth W, Menzel D (1999) *Chem Phys Lett* 315:194
63. Schiffer A, Jakob P, Menzel D (1997) *Surf Sci* 389:116
64. Fuggle JC, Madey TE, Steinkilberg M, Menzel D (1975) *Surf Sci* 52:521
65. Friedrich KA, Geyzers KP, Marmann A, Stimming U, Vogel R (1999) *Z Phys Chem* 208:137